
Distance Measurement Error Reduction Analysis for the Indoor Positioning System

TARIQ JAMIL SAIFULLAH KHANZADA*, JAVED ALI BALOCH**, AND SANIA BHATTI***

RECEIVED ON 31.05.2012 ACCEPTED ON 18.09.2012

ABSTRACT

This paper presents the DME (Distance Measurement Error) estimation analysis for the wireless indoor positioning channel. The channel model for indoor positioning is derived and implemented using 8 WLAN (Wireless Local Area Network) antennas system compliant to IEEE 802.11 a/b/g standard. Channel impairments are derived for the TDOA (Time Difference of Arrival) range estimation. DME calculation is performed over distinct experiments in the TDOA channel profiles using 1,2,4 and 8 antennas deployed system.

Analysis for the DME for different antennas is presented. The spiral antenna achieves minimum DME in the range of 1m. Data demographics scattering for the error spread in TDOA channel profile is analyzed to show the error behavior. The effect of increase in number of recordings on DME is shown by the results. Transmitter antennas behavior for DME and their standard deviations are depicted through the results, which minimize the error floor to less than 1 m. This reduction is not achieved in the literature to the best of our knowledge.

Key Words: DME, Time Difference of Arrival, Indoor Positioning Systems, Wireless Channel.

1. INTRODUCTION

Distance measurement error reduction is the key issue concerned in the positioning systems. In outdoor environments the error ranges are loosely bound while specific accuracy is the main concern in the indoor systems. Noise and interference are the main factors, which degenerate the efficiency and accuracy [1]. However, a number of navigational systems like GPS (Global Positioning System) [2] have been proposed throughout the world like a fully functional navigation constellation GLONASS (GLObal'naya NAvigatsionnaya

Sputnikovaya Sistema) [3], QZSS (Quasi-Zenith Satellite System), an enhancement for GPS [4] covering Japan, and the IRNSS (Indian Regional Navigational Satellite System) [5] developed by Indian space research organization.

Various techniques are implied in order to meliorate the estimation in the multi-path channel, [1,6] which include UWB (Ultra Wide Band), RT (Ray Tracing), and Multi-hop WSN [7-9]. The location finding and its DME is based on the location metric adopted for estimation. Proximity and

* Associate Professor, Department of Computer Systems Engineering, Mehran University of Engineering & Technology, Jamshoro.
** Assistant Professor, Department of Computer Systems Engineering, Mehran University of Engineering & Technology, Jamshoro.
*** Assistant Professor, Department of Software Engineering, Mehran University of Engineering & Technology, Jamshoro.

finger printing are commonly used and can be subcategorized under RSS (Received Signal Strength) and sometimes under TOF (Time of Flight) [10]. The other metrics location sensing include Angle, Time and TDOA. The accuracy of TDOA is better than that of RSS [11]. The geometric principles of the TOA and TDOA location methods are the same for the unilateral (fixed receiver) and the multilateral (moving receivers) systems, both requiring a channel to communicate. The channel is a vital and integrated component of the wireless communication system. Its design governs the variety of performance and value of any system under consideration. Therefore, accurate knowledge of the channel is either required or to be estimated while the design of the wireless communication system is initiated. This is termed as channel characterization. For the indoor positioning used in this article, we have focused on estimating the channel, which is very random with the coarse, and intriguing situations. Multi-path reception is a characteristic of the wireless channel. With multi-path channel various vital impairments are associated which are Doppler spread, delay spread, shadow fading, propagation path loss, time dispersion and the other parameters. Consequent section derives the model for multi-path channel and then some of its important impairments.

In the paper the introduction is followed by the section wireless communication channel model, which describes the model, its impairments and TOA/TDOA channel profile. In Section 3, the deployment of an indoor positioning system and experimental details are discussed. Section 4 includes the results obtained and finally the paper is concluded in Section 5.

2. WIRELESS COMMUNICATION CHANNEL MODEL

We can simply model the wireless channel in frequency domain by taking the ratio of the transmitted and the

received signals, which is known as the CTF (Channel Transfer Function). Applying the time domain IFFT (Inverse Fast Fourier Transform) produces the CIR. If a signal is transmitted in the wireless communication environment, the incident field $E(\omega, r, t)$ caused by the received signal is a function of the angular frequency ω , the distance r and the time t . Assuming that the signal is propagated in free space, the received electromagnetic wave can be shown as:

$$E(\omega, r, t) = E_0 e^{j\omega t - j\beta r} \quad (1)$$

where β is called phase factor and represented by:

$$\beta = \frac{\omega}{c} \quad (2)$$

where c is the free space speed of light. The received signal will have a time delay τ which depends on range r . The relation between time delay and the distance can be written as follows:

$$\tau = \frac{r}{c} \quad (3)$$

The electric field now can be written as:

$$E(\omega, r, t) = E_0 e^{j\omega t - j\omega \tau} \quad (4)$$

The signal is received through multiple number of paths in a typical wireless communication system. These paths, shown in Fig. 1(a), are caused by the numerous reflections, diffractions and scattering by the different objects lying between the transmitter and the receiver.

A typical wireless channel generally comprises these paths and its CIR can be represented by a tapped delay module, shown in Fig. 1(b). Multi-path interference introduces the path delay and fading in the received signals. The fading is modelled as a number of sinusoids [12], each of which corresponds to different scattered and reflected rays. The CIR for this model can be written as:

$$h(\tau) = \sum_{l=1}^L h_l \delta(\tau - \tau_l) \quad (5)$$

where h_l and τ_l are the propagation path amplitudes and the delays respectively. Each multi-path component will have different phase resulting in constructive or destructive interference due to the delay. The CTF is calculated by employing the FT (Fourier Transform) to the CIR with respect to the delay as follows:

$$H(f) = \int_{-\infty}^{\infty} h(\tau) e^{-j2\pi f \tau} d\tau = \sum_{l=1}^L h_l e^{-j2\pi f \tau_l} \quad (6)$$

Equation (1) shows the frequency-selectivity, which is a transfer function characteristic property of a multi-path radio channel. This means that due to the multi-path interference the channel is frequency selective fading. Fig. 1(c) mimics this effect. The multi-path parameters can be calculated by CIR. If a high data rate stream is transmitted over the frequency selective channel, multiple data symbols interfere with each other, making the data detection difficult. Therefore, some design technique is needed to overcome this situation.

2.1 Time Varying Wireless Channels

If there is a relative movement with random speed and will be direction between source and destination, the frequency shift is caused due to the Doppler's effect [13]. When the receiver is moving, the Doppler shift f_d is given by [12]:

$$f_d = \frac{v}{\lambda} \cos \alpha \quad (7)$$

where v is the velocity of the moving receiver and α is the angle of arrival of the direction of incoming horizontal signal at frequency f . Thus the Doppler shift associated with the received signal frequency f by the factor f_d as $f = f + f_d$. Assuming that L multi-path components reach the receiver, then the time variant CTF $H(t, f)$ is derived as:

$$H(t, f) = \sum_{l=1}^L h_l e^{j2\pi f d t} e^{-j2\pi f \tau_l} \quad (8)$$

The corresponding CIR with respect to τ and f_d is given by:

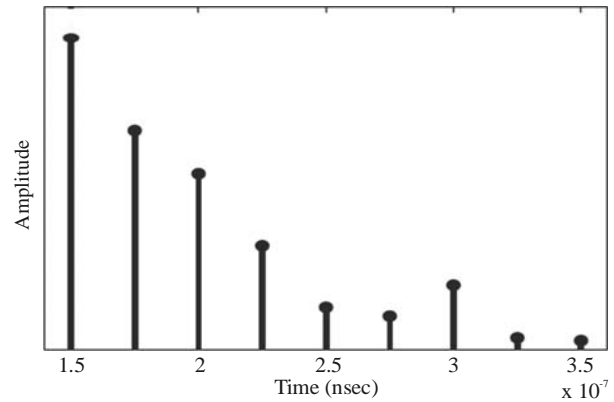


FIG. 1(a) MULTI-PATHS CIR

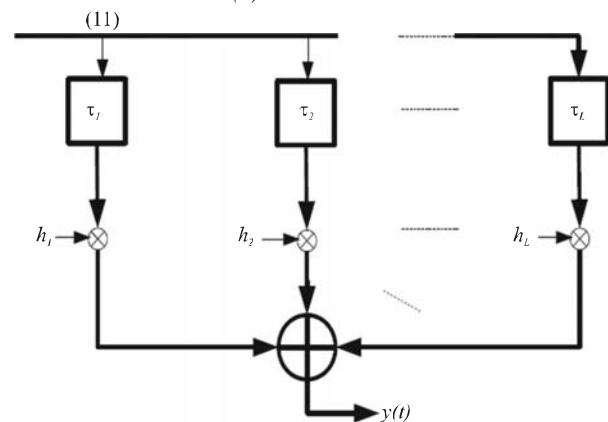


FIG. 1(b). EQUIVALENT TAPPED DELAY LINE CHANNEL MODEL

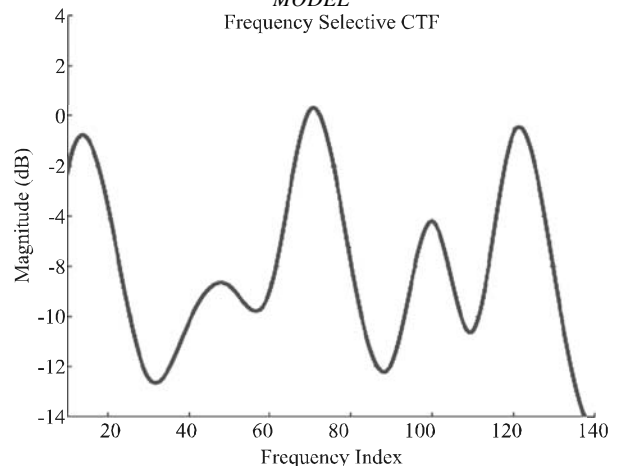


FIG. 1(c) FREQUENCY SELECTIVE CTF

$$h(\tau, f_D) = \sum_{l=1}^L h_l \delta(\tau - \tau_l) \delta(f_D - f_{dl}) \quad (9)$$

where τ_l and f_{dl} are the delay and the doppler shift of the corresponding path l .

2.2 Statistical Channel Model

WSSUS (Wide Sense Stationary Uncorrelated Scattering) is a simple channel, introduced by Bello [14] and used in many channels. In this model the autocorrelation function of $h(\tau, t)$ is defined as follows:

$$\Phi_h(\Delta\tau, \Delta t) \sigma(\Delta\tau) = E[h^*(\tau, t) h(\tau + \Delta\tau, t + \Delta t)] \quad (10)$$

If we set the difference Δ_t to zero, the resulting autocorrelation function describes the channel's time spread. This function is known as the delay power spectrum. The equivalent autocorrelation function in frequency domain of the WSSUS is defined as following:

$$R(\Delta_f, \Delta_t) = E[H^*(f, t) H(f + \Delta_f, t + \Delta_t)] \quad (11)$$

where $(.)^*$ represents the complex conjugate. The above correlation matrix depends only on the frequency Δ_f and on the time Δ_t separations. In other words, the time-variant channel transfer function is wide-sense stationary with respect to both variables t and f [15-16]. The concept of the uncorrelated scattering means that the phase and attenuation of a propagation path are respectively uncorrelated with each others. The autocorrelation function of the CTF can now be separately computed in the time and frequency domains as follows:

$$R(\Delta_f, \Delta_t) = R_f(\Delta_f) R_t(\Delta_t) \quad (12)$$

where $R_f(\Delta_f)$ and $R_t(\Delta_t)$ are the frequency and the time correlation functions of CTF, respectively.

To characterize the indoor channel, the following parameters have to be estimated:

- (i) *Doppler Power Spectral Density and Coherence Time*: The delay power spectral density $\Phi_l(\tau)$ is obtained by integrating the scattering function $\Phi(\tau, f_d)$ with respect to f_d . The Doppler power spectral density $\Phi_{fd}(f_d)$ is obtained by integrating the scattering function $\Phi(\tau, f_d)$ with respect to τ . By finding the Doppler spread the coherence time T_c can be estimated. They are inversely proportional to one another [13]:

$$T_c \approx \frac{1}{f_d} \quad (13)$$

The coherence time gives the measure for the channel's time variation. It is the time span over which the channel remains approximately constant.

- (ii) *DPF (Power Delay Profile)*: PDF is the power response of the channel and is defined by:

$$p(\tau) = |h(\tau)|^2 \quad (14)$$

- (iii) *RMS (Root Mean Square) Delay*: RMS delay is the PDP second central moment's square root given as shown as:

$$\tau_{rms} = \sqrt{\frac{\int_{-\infty}^{\infty} (t - \tau_m)^2 p(t) dt}{\int_{-\infty}^{\infty} p(t) dt}} \quad (15)$$

where τ_m is the mean access delay defined by:

$$\tau_m = \frac{\int_{-\infty}^{\infty} t p(t) dt}{\int_{-\infty}^{\infty} p(t) dt} \quad (16)$$

If the parameters are known, the τ_{rms} , can be calculated as [13]:

$$\tau_{rms} = \sqrt{\tau^2 - (\bar{\tau})^2} \quad (17)$$

where

$$\overline{\tau^2} = \frac{\sum_{k=1}^L \tau_k^n a_k^2}{\sum_{k=1}^L a_k^2} \quad (18)$$

RMS delay spread is important since it is used to quantify the time dispersion of wide-band indoor multi-path channel, and consequently the ISI. The RMS delay spread defines the maximum reliable data rate that can be used in the indoor WLAN without ISI.

- (iv) *Coherence Bandwidth Bc*: The correlated signal propagation statistical average bandwidth of the channel is known as the coherence bandwidth. Coherence bandwidth is inversely proportional to RMS delay spread and can be approximated by:

$$B_c \approx \frac{1}{50\tau_{rms}} \quad (19)$$

- (v) *Ricean Factor K*: The fading is characterized as Ricean the in indoor channels for the Line of Sight path is available. It is a factor that is used to define a Ricean channel. It is the ratio between the LOS signal power and the multi-path components power denoted by K:

$$K = \frac{h_{max}^2}{P_o - h_{max}^2} \quad (20)$$

where $h_{max} = \max(h_l), l \in [1, \dots, L]$ and $P_o = \sum_{l=1}^L h_l^2$ is the total power. The problem reduces to estimate these parameters. The relation between these functions is summarized in Fig. 2.

If d is the distance between the transmitter and the receiver, we can rewrite Equation (5) of the CIR as:

$$h_d(t) = \sum_{i=1}^{L_p} \beta_i^d \delta[t - \tau_i^d] \quad (21)$$

where L_p is multi-path components, $\beta_i^d = |\beta_i^d| e^{j\phi_i^d}$ and τ_i^d represents the i^{th} path random complex amplitude and random propagation, respectively. Having finite bandwidth ω ; the transmitted signal $x^\omega(t)$ and the received signal $r_d^\omega(t)$ can be modelled as:

$$r_d^\omega(t) = \int_{-\infty}^{+\infty} x^\omega(\tau) h_d(t - \tau) d\tau \quad (22)$$

2.3 TOA Estimation from the Channel Profile

The TOA of the direct LOS path between the transmitter and the receiver indicates the distance range. The TOA of the FDP (First Detection Peak) is used as an estimate TOA of the direct LOS path denoted by $\hat{\tau}_{1,\omega}$. The estimated range is calculated as $\hat{d}_\omega = c \times \hat{\tau}_{1,\omega}$, where c is the light's speed.

In an ideal situation the estimated and actual direct paths are the same, whereas the multi-path channel causes an estimation error. This estimation error is known as DME. The DME can be calculated as:

$$\varepsilon_{1,\omega} = |\hat{d}_\omega - d| \quad (23)$$

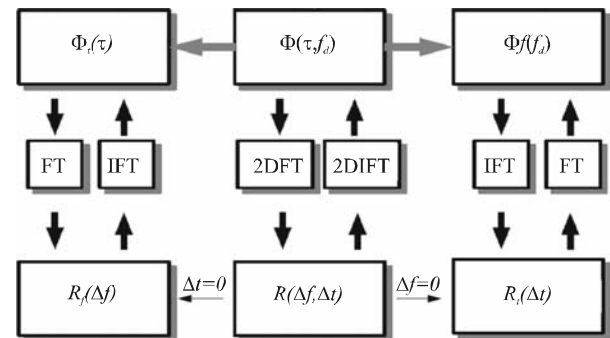


FIG. 2. RELATIONSHIP BETWEEN THE TIME VARYING SYSTEM CHANNEL PROFILE FUNCTIONS

3. TDOA INDOOR POSITIONING DEPLOYED SYSTEM

Our deployed system focuses from 4 antennas TDOA system to 8 transmitters including one reference antenna. We have tested various recorded data packages using variants of the MP algorithm combined with some old and new model order criteria. The parameter for the antennas used for implementing the positioning system is shown in Table 1. The system is a unilateral system using the TDOA method because we have used the 8 fixed transmitter antennas to estimate the position of the static and the dynamic receiver by measuring their TDOA. In order to enhance and validate the system, the measurements are taken at two different buildings. The diagram for the system setup with 8 transmitted antennas is shown in Fig. 3 and the observed ranges and delays for various experiments are shown in Table 2. The data sets are recorded for different points in the ground floor and the first floor of the building. Some receiver points were on the stairs and on the second floor. The list of receiver measurement points along with their X, Y and Z coordinates is shown in Table 3.

TABLE 1. INDOOR ANTENNAS USED AND THEIR PROPERTIES

No.	Name of Antenna	Frequency Range	Antenna Gain
1.	IESK	2.4Ghz-2.6Ghz	9dBi
2.	IESK-Spiral	800Mhz-18Ghz	8dBi
3.	DWL M60AT	2.4Ghz-2.5Ghz	6dBi
4.	Hyperlog	700Mhz-64Ghz	4dBi

TABLE 2. OBSERVED RANGES AND DELAYS FOR VARIOUS EXPERIMENTS

No.	For Initial Experiments (Unilateral System)			No.	For Multilateral System		
	Observation	Range (m)	Delay (nSec)		Observation	Range (m)	Delay (nSec)
1.	CSE-UL1	16.75	415	1.	CSE-MA1	10.6	0
2.	CSE-UL2	30.25	415	2.	CSE-ML2	6.10	0
3.	CSE-UL3	18.30	350	3.	CSE-ML3	30.5	0
4.	CSE-UL4	40.00	350	4.	CSE-ML4	16.75	0
5.	CSE-UL5	7.5	350	5.	CSE-ML5	20.25	0
6.	CSE-UL6	15.5	225	6.	CSE-ML6	5.25	0
7.	CSE-UL7	20.25	225	7.	CSE-ML7	27.5	0
8.	CSE-UL8	26.661	225	8.	CSE-ML8	9.10	0

Different data sets are prepared gradually for estimation of the receiver range. Initially static measurement data sets are prepared to validate the basic method. Later on the dynamic recordings are carried out using a selected direction in the corridors of the building at different floors. The plan of the observed building is shown in Fig 4(a) and the direction of the receiver movement for the dynamic data recordings along with 8 transmit antennas positions are shown in Fig. 4(b). The list of all data sets used in to implement the positioning system with the number of points in a data set, resolution of recording per point and the number of antennas used for the recording is shown in Table 4.

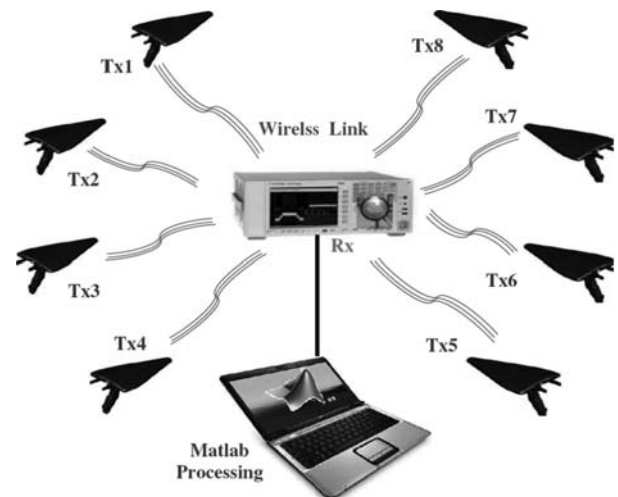
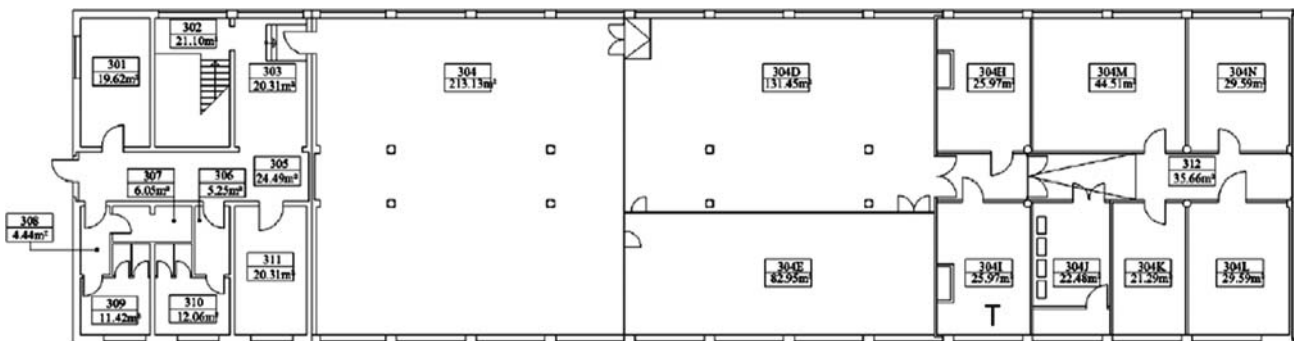


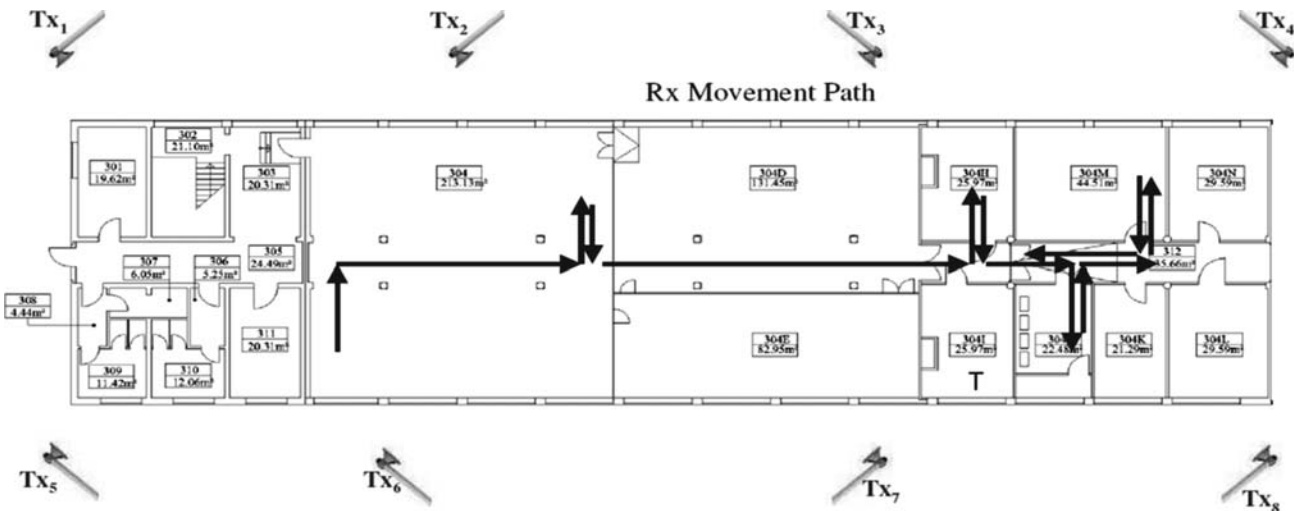
FIG. 3. INDOOR POSITIONING SYSTEM SETUP

TABLE 3. RECEIVER POSITION COORDINATES

No.	Dimension-X	Dimension-Y	Dimension-Z	No.	Dimension-X	Dimension-Y	Dimension-Z
1.	145	50	-0.5	16.	145	30	7.5
2.	151.5	30	-0.5	17.	145	20	7.5
3.	158.5	30	-0.5	18.	145	50	7.5
4.	166.5	50	-0.5	19.	145	30	7.5
5.	145	30	1.25	20.	145	20	7.5
6.	151.5	20	1.25	21.	145	50	7.5
7.	158.5	30	1.25	22.	145	20	7.5
8.	166.3	50	1.25	23.	145	30	7.5
9.	145	20	4.5	24.	145	50	7.5
10.	151.5	30	4.5	25.	145	20	7.5
11.	158.5	50	4.5	26.	145	30	7.5
12.	166.5	20	4.5	27.	145	50	7.5
13.	155.5	30	-0.562	28.	145	30	7.5
14.	165	50	-0.141	29.	174.476	30	7.5
15.	99.785	64.426	-0.087	30.	184.441	30	7.5



(a). THE PLAN OF THE TEST AREA WITH MEASUREMENTS



(b). RECEIVER MOVEMENT PATH AND TRANSMITTER ANTENNA POSITIONS

FIG. 4. INDOOR POSITIONING SYSTEM EXPERIMENT TEST BUILDING PLAN

4. RESULTS ANALYSIS

Different experiments have been performed to validate the antennas listed in Table 1. Fig. 5 shows results comparison from these antennas. It is clear from Fig. 5 that IESK Spiral Antenna estimates the original ranges with minimum DME due to its spiral design the optimal results are obtained. The DME is reduced to less than 1m in a range of 30m transmission. Fig. 8 shows the Data demographic scattering for the DME.

Fig. 6 shows the data demographics scattering for the error spread in TDOA channel profile. It is evident from the figure that the error is spread up to 100, 50 and -50m for the x,y and z dimensions. This roughly predicts that the movement along x dimension produces comparatively more error and the DME is observed growing in x dimension for the TDOA channel profile.

Fig. 7 shows the estimation accuracy effects governed by the number of recordings of the experiments. Increase in number of recordings increases the estimation accuracy thus reduces the DME. A detailed observation of the figure clarifies that the DME floor is decaying while we move with the horizontal axes to increase the number of recording per experiment in the TDOA channel profile.

Fig. 8 depicts the fact that increase in number of transmitter antennas increases the accuracy and decreases the DME. The 8 Antennas case matches closer estimates than all other cases in all the estimation range while Fig. 9 portrays the respective standard deviations for all the cases. The

minimum standard deviation verifies that the most accurate estimates are achieved by the 8 antennas case in the TDOA channel which reduces the DME less than 1m.

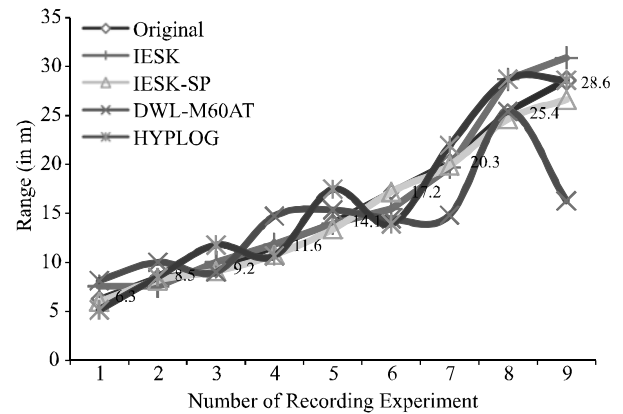


FIG. 5. INDOOR ANTENNAS PERFORMANCE COMPARISON
Data Demographics Scattering

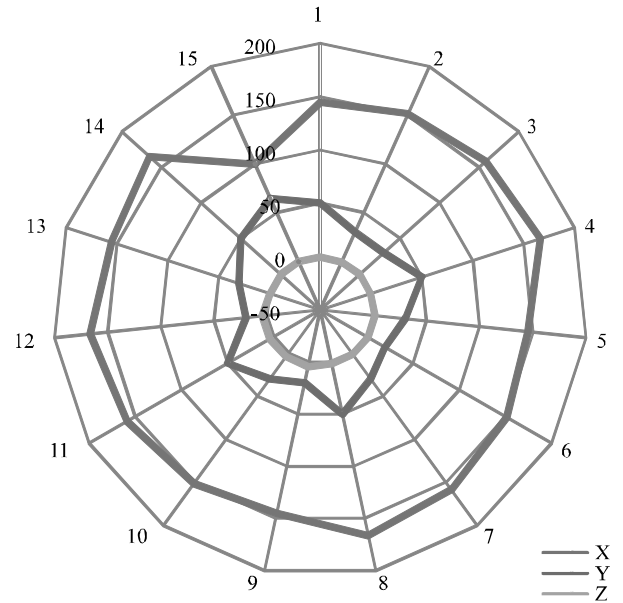


FIG. 6. DATA DEMOGRAPHIC SCATTERING FOR DME

TABLE 4. THE OBSERVED EXPERIMENT DATA

No.	Observation	Resolution	Iteration	Nature	No. of Antennas
1.	CSE-ML41	12	25	Static	1
2.	CSE-ML81	18	400	Static	2
3.	CSE-ML82	25	150	Static	4
4.	CSE-ML83	25	180	Static	4
5.	CSE-ML8G	Numerous	400	Dynamic	6
6.	CSE-ML8G	Numerous	600	Dynamic	6
7.	CSE-ML81	Numerous	1000	Dynamic	8
8.	CSE-ML8G2	Numerous	1200	Dynamic	8

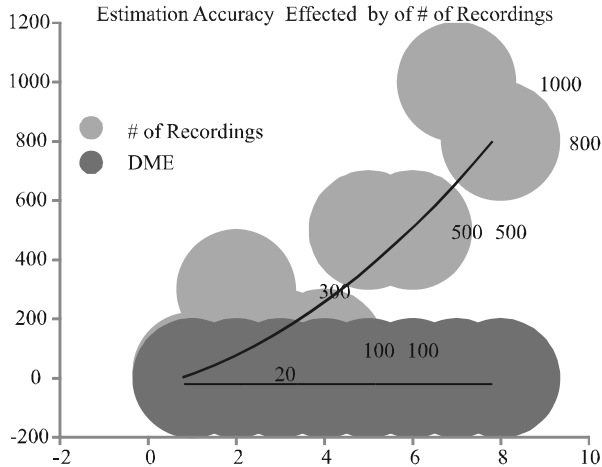


FIG. 7. ESTIMATION ACCURACY W.R.T # OF RECORDINGS

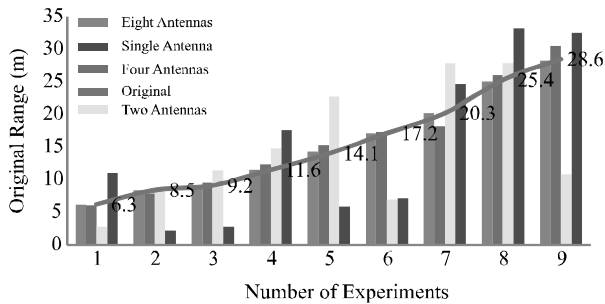


FIG. 8. COMAPRISION OF 1,2,4,8 ANTENNAS ESTIMATES

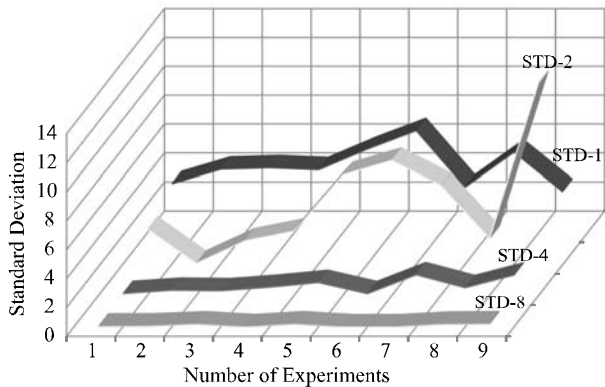


FIG. 9. STANDARD DEVIATIONS OF 1,2,4,8 ANTENNAS ESTIMATES

5. CONCLUSION

We have presented the DME estimation analysis for the wireless indoor positioning channel. The channel model for indoor positioning is derived and implemented using 8 WLAN antennas system. Channel impairments are derived for the TDOA range estimation. DME calculation is

performed over distinct experiments in the TDOA channel profiles using 1,2,4 and 8 antennas deployed system. Analysis for the DME for different antennas is presented. Minimum DME in the range of 1m is achieved by the spiral antenna. Data demographics scattering for the error spread in TDOA channel profile is analyzed to show the error behavior. The effect of increase in number of recordings on DME is shown by the results. Transmitter antennas behavior for DME and their standard deviations are depicted through the results which minimize the error floor less than 1m.

ACKNOWLEDGMENTS

We are thankful to Mehran University of Engineering & Technology, Jamshoro, Pakistan, and HEC (Higher Education Commission), Pakistan, for providing support to this research.

REFERENCES

- [1] Li, X., "Collaborative Multi-Sensor Tracking in Mobile Wireless Sensor Networks", International Journal of Sensor Networks, Volume 8, No. 3/4, 2010.
- [2] Khanzada, T.J.S., Ali, A.R., and Omar, A.S., "Time Difference of Arrival Estimation Using Super Resolution Algorithms to Minimize Distance Measurement Error for Indoor Positioning Systems", IEEE International Multitopic Conference, pp. 443-447, 23-24 December, 2008.
- [3] "Glonass summary," Space and Tech, Technical Report, December, 2007.
- [4] Kogure, "Presentation at the 47th Meeting of the Civil Global Positioning System Service Interface Committee (CGSIC)," Bureau des Longitudes, 23, Quai Conti, 75006 pp. 62-63, Paris France, September 25, 2002.
- [5] Space, I., "SATNAV Industry Meet 2006. ISRO Space India Newsletter," April-September, 2006.
- [6] Dumont, L., Fattouche, M., and Morrison, G., "Super Resolution of Multipath Channels in a Spread Spectrum Location System", Electronic Letter, Volume 30, pp. 1583-1584, Septmber, 1994.

- [7] Fontana, R.J., and Gunderson, S.J., "Ultra-Wideband Precision Asset Location System", IEEE Conference on UWB Systems and Technologies, pp. 147-150, Baltimore, MD, 2002.
- [8] Alsindi, N., Alavi, B., and Pahlavan, K., "Spatial Characteristics of UWB TOA Based Ranging in Indoor Multipath Environments", IEEE International Symposium on Personal Indoor and Mobile Radio Communications, pp. 1-6, Athens, Greece, September, 2007.
- [9] Chang, C., and Sahai, A., "Cramer-Rao-Type Bounds for Localization", EURASIP Journal on Applied Signal Processing, pp. 1-13, 2006.
- [10] Caffery, J.J., "Wireless Location in CDMA Cellular Radio Systems", Kluwer Academic Publishers, 2000.
- [11] Hatami, A., "Application of Channel Modeling for Indoor Localization Using TOA and RSS", Ph.D. Dissertation, Worcester Polytechnic Institute, 2006.
- [12] Hwang, J., and Winters, J., "Sinusoidal Modeling and Prediction of Fast Fading Processes", IEEE GLOBECOM, pp. 892-897, November, 1998.
- [13] Khanzada, T.J.S., Memon, S., and Hashmani, A.A., "A Novel Method to Implement the Matrix Pencil Super Resolution Algorithm for Indoor Positioning", Mehran University Research Journal of Engineering & Technology, Volume 30, No. 4, pp. 625-634, Jamshoro, Pakistan, October, 2011.
- [14] Bello, P., "Characterization of Randomly Time-Variant Linear Channels", IEEE Transactions on Communication System, Volume 11, pp. 360-393, 1963.
- [15] Proakis, J.G., "Digital Communications", McGraw-Hill International Editions, 3rd Edition New York, 1995.
- [16] Alsindi, N., "Indoor Cooperative Localization for Ultra Wideband Wireless Sensor Networks", Ph.D. Dissertation, Electrical and Computer Engineering, Worcester Polytechnic Institute, April, 2008.